Simulating Interior Radiant Energy for the Design and Prototyping of an Indoor Solar PV Lamp

Verkou, M.H.; Ziar, H.; Isabella, O.; Zeman, M.

Publication date
2020

Document Version
Final published version

Published in
proceedings of the 37th European Photovoltaic Solar Energy Conference and Exhibition

SIMULATING INTERIOR RADIANT ENERGY FOR THE DESIGN AND PROTOTYPING OF AN INDOOR SOLAR PV LAMP

Maarten Verkou, Hesan Ziar, Olindo Isabella, and Miro Zeman
Delft University of Technology, Photovoltaic Materials and Devices group, Delft, the Netherlands
Email: m.h.verkou@tudelft.nl, Phone: +316 305 82 568

ABSTRACT: The increasing development of photovoltaic (PV) technologies allows for more feasible PV products, that can split the fixed big electrical infrastructure into smaller mobile systems, suitable for future smart buildings. This research, investigates opportunities for interior PV (IPV) products, that harvest indoor ambient light. The outcome is a working prototype of a standalone indoor solar lamp. An indoor light simulation model is presented and validated for two rooms in Delft with absolute error of 10% compared to measurements over five days per room. The prototype consists of a tailor-made, foil-to-foil laminated PV module, consisting of 36 pieces of laser cut SunPower interdigitated back contact (IBC) cells. At standard test conditions, a maximum DC output of 35.9 Wp was measured, corresponding to a module efficiency of 20.3%. Furthermore, a charge controller with maximum power point tracking algorithm was used to charge a 12 V polymer lithium-ion battery pack. The combination of pyroelectric infrared (PIR) motion sensor detector and a light sensor module assures a conservative use of a 2.4 W strip of light emitting diodes (LED).
Keywords: Indoor photovoltaics (IPV), interior light simulation, RADIANCE, PV module design, prototyping, SunPower IBC technology, laser cutting

1 INTRODUCTION

Look into any modern living room and you will find that almost every electrical device is cable connected, apart from some low power consumption devices, like the remote control, typically using less than a few milliwatts of power. In this range, photovoltaic cells have already found a home over 40 years ago, for example in the famous solar pocket calculators [1]. For high power consumption devices, like televisions, the electrical infrastructure inside a building dictates the furnishing of the room. This can restrict the organization of medium power consumption devices, like decorative lamps, inside the room. The development of PV cell efficiency opens a door to make such devices cable free.

This research includes the design and prototype a cable-free, easy-to-install solar powered lamp for interior spaces. The aim of this paper is to find out if it is feasible to create such a product with readily available components and PV cell technologies. The product has to be aesthetically pleasing as well as functional for the environment in which it is designed. The target group for the product are ordinary Dutch households, so research will be done there on the availability of radiant energy. This will then be used to determine the required shape and size of the solar module to produce the desired power for a light emitting diode (LED) light source.

The scientific relevance of this paper is that insights and recommendations are provided for indoor PV products. The research on the available radiant energy provides a method that is suitable for any light simulation that determines the irradiance inside buildings. Emphasis has been laid on reducing the computational effort, whilst maintaining sufficient accuracy. The results will be useful for any researcher that feels frustrated by the long run-time of ray-tracing simulations. A more practical relevance can be found in the process of laser cutting of 50 SunPower IBC cells into three equal area parts. From this, valuable experience is gained in that aspect.

Chapter 2 describes the preparation of the simulation environment test setup for pyranometer measurements. In Chapter 3, the new model is validated and used to analyze multiple room characteristics. Finally, the final specifications of the prototype are shown in Chapter 4.

2 METHODOLOGY

An accurate indoor simulation is needed to identify the best performing indoor areas, which also dictates the shape and properties of the prototype. This was done for two rooms, namely a household living room and a university office room. The former has its main window facing almost south (167 degrees from north) and the latter is facing east-northeast (67 degrees from north).

2.1 Simulation approach

The room and its surroundings are reproduced in the open source 3D modelling program Blender, using satellite images and a simple tape measure. As can be seen in Figure 1. Only main room geometries are considered, furniture can often be neglected [2]. Using an external add-on [3] in Blender, the irradiance along every relevant surface is calculated with the RADIANCE light simulation tool [4]. The tool works with a backwards ray-tracing algorithm, which can be computationally heavy. So, with a sensitivity study, the simulation time interval and accuracy (here: amounts of rays traced) are optimized for fast and accurate computation.

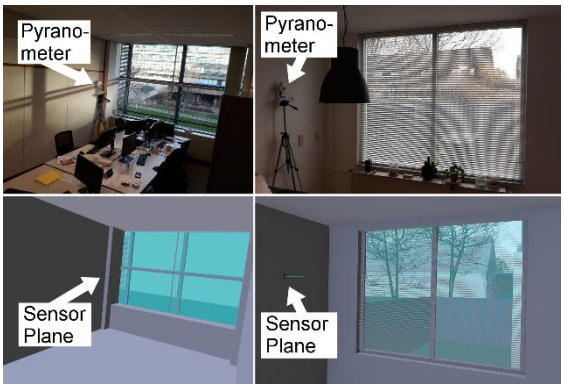

Figure 1: The top left and right images show an office room on the second floor of the EWI faculty at the Delft University of Technology and a living room in the South of Delft, respectively. Below them are their recreated 3D models. The pyranometer position and corresponding sensor plane are annotated.

Within the Blender program, one can choose between three sky types: sunny, partly cloudy and cloudy, corresponding to three CIE standard skies [5]: clear, overcast, and intermediate sky type. Remaining settings were left to their default value.

It was found that cleaner skies require a shorter time interval to account for the shading effects from nearby objects. It was required to be as low as 1 minute when the sun hits the sensor directly, otherwise 1 hour is sufficient. When there is not much light in the indoor scene, the accuracy of the simulation needs to be higher, because a ray send randomly from the sensor is less likely to find a light source.

2.2 Experimental setup

Measurements were done with a thermopile pyranometer (CMP3) from Kipp&Zonen, to find the incident irradiance. A tripod stand was used to keep the pyranometer at the right position, as can be seen in Figure 1. The lighting simulation tool RADIANCE is used in this research. It calculates the irradiance for each single ray in W/m^{2}sr by using RGB colours, meaning that the visible irradiance is calculated. After that a constant factor is used to estimate the full irradiance value for the whole spectrum [a26]. So, to compare with this value, a pyranometer is needed that has a long range, and the CMP3 pyranometer is very suitable for this, because it has a spectral range from 300 to 2800 nm.

2.3 Sky type determination

Weather data from the KNMI (Koninklijk Nederlands Meteorologisch Instituut) was used to classify the sky conditions for every hour. Three criteria, the cloud cover in okta, sun time in hr/day and rain time in hr/day, were collected from the three most nearby weather stations. If the cloud cover was less than 4.0 okta and the sun had shown for at least half an hour during that hour, the sky was still considered sunny. This is also when the sun has shown itself for more than 8 hours, even with a cloud cover of 7.0 or less okta. When the cloud cover was higher than 7 okta and the sun was visible for 2 or less hours, then the sky for that hour is close to full overcast. In any other case, the sky type was considered intermediate.

2.4 Full year simulation

To simulate a full year, the first day in every month was simulated. This was done for each of the three standard sky types. Instead of checking the weather data every hour of the year to determine the sky type at that hour, historical weather data of the past 5 years is used to get an overview of how many hours of the day each sky type occurs. Only the hours between sunrise and sunset are considered in this analysis. It can be seen in Figure 2, that more often than not the sky is cloudy in the Netherlands.

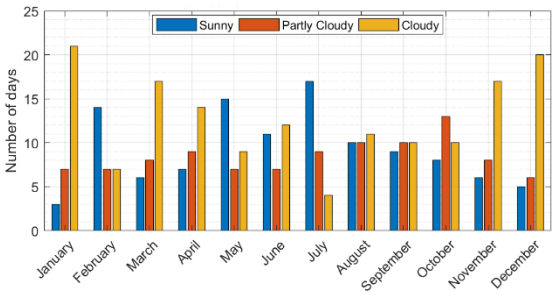

Figure 2: Number of hours in a year of the three standard sky types.

Overall, 40% of the time the sky is completely overcast and only 28% of the time is it clear. The remaining 32% is defined as intermediate sky. With these ratios the average irradiance curve for each month can be calculated as the weighted sum of the three base curves. Eventually, this was done for different global orientations of the room and different spots and orientations of the sensor plane inside the room.

2.5 PV cell efficiency in low-intensity light

The power conversion efficiency (PCE) of multiple PV technologies in low irradiance conditions is taken into account to find the best performing cell technology to use in the module. Randall [5] investigated over twenty solar cell technologies and deducted the parameters a and b to calculate the efficiency in percentages. The model assumes a linear curve on the logarithmic scale for the efficiency below 100 W/m2 and the relation between the parameters can be seen in Equation 5.1.

$$\eta(\%) = a \ln G + b \qquad (2.1)$$

The values for the parameters a and b are technology specific and G is the irradiance. Note, in the research of Randall it is assumed here that the light source is a dimmed AM1.5 spectrum. This is of course not the case for each time of the day across the year. The spectrum of light depends on a lot of factors, for now, it was considered out of the scope of this research.

In this analysis, it has been decided to pick only the best performing cell from the monocrystalline silicon (mono-c-Si), multicrystalline silicon (mc-Si) and amorphous silicon (a-Si) classes. Cells with a low a/b ratio are expected to perform best in low irradiance conditions. The characteristics of the chosen cells are shown in Table 1.

Table 1: Specifications of the three chosen solar cell technologies. Note, Tessag has had a name change to RWE.

Technology	Supplier	a	b
mono-c-Si	BP Solar	1.71	2.58
mc-Si	EFG, Tessag (RWE)	2.33	0.48
a-Si	Tessag (RWE)	0.43	5.41

Using the parameters a and b in Equation 2.1, the performance can be calculated, as shown in Figure 3.

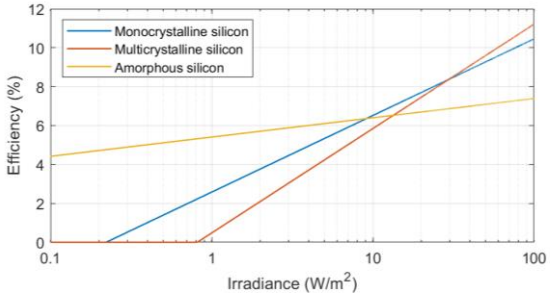

Figure 3: PV cell efficiency of three cell technologies given in Table 1, using Equation 2.1.

It can be seen that for lower intensity light, monocrystalline silicon will outperform multicrystalline silicon below 30 W/m^2 and amorphous silicon will outperform both below 9 W/m^2.

3 RESULTS AND DISCUSSION

Results were gathered for both of the rooms introduced in the previous chapter. In Section 3.2 of the discussion, only the results of the office room are shown.

3.1 Artificial light

From the early measurements, it became apparent that focusing on both artificial and outdoor light, would be conflicting and results in poor performance on both sides. Reason (1) being the spectral differences of the two light sources and (2) the direction of light coming often from opposing sides. It was found that the irradiance of artificial light is approximately 0.5 W/m^2, for ordinary households and office rooms.

3.2 Indoor light simulation validation

Figure 4 shows the first three days of a five-day group of measurements in the office room during a week in November.

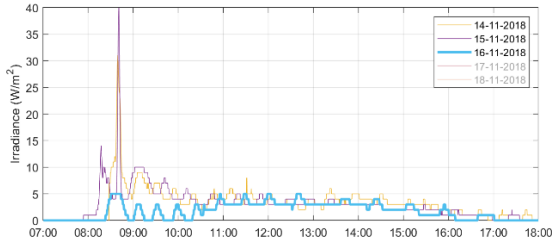

Figure 4: Results of pyranometer measurements for office week in November.

A general pattern can be seen that is a direct result of the main geometry of the room. Direct light only enters the room in the morning between 8 AM and 10 AM. It is in this period that large variations occur due to incidental shading caused by the cross-beams and blinds of adjacent rooms, which can be seen in Figure 1.

Instead of having one small sensor plane, like is shown in Figure 1, the simulation tool also allows the user to calculate the irradiance for the entire surface area on the wall. This was done for the whole day to get a good idea of the light entering the room. Three snapshots where made and are shown in Figure 5.

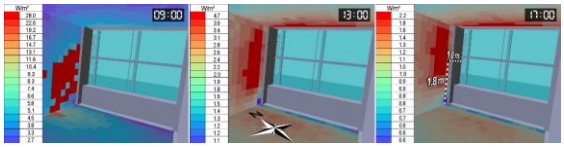

Figure 5: Three snapshots of a daily simulation for the office room during partly cloudy conditions in September, at 9 AM, 1 PM and 5 PM. The color map shows the irradiance values. Note, that they change during each time step to amplify the difference in color.

This clearly shows the pattern, with light entering the room directly in the morning with an intensity up to 30 W/m^2. For the remainder of the day, the intensity does not go above 5 W/m^2. It also shows that the intensity is high in a narrow column along the height of the window, and drops of sharply deeper into the room for most of the day.

Now we will consider only the pyranometer/sensor spot on the wall, which is highlighted on in Figure 5 at 5 PM. The results from the simulation with the three standard sky types are shown in Figure 6. They are referred to as the three base simulations

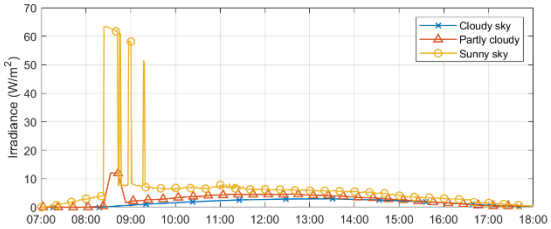

Figure 6: Three base simulations for office room. Each of the three sky conditions can be found in the graph.

The simulated irradiance curves per day of testing were now created by determining the sky at each hour using KNMI data. The results can be compared with the measurements on same days. The resulting average plots can be seen in Figure 7.

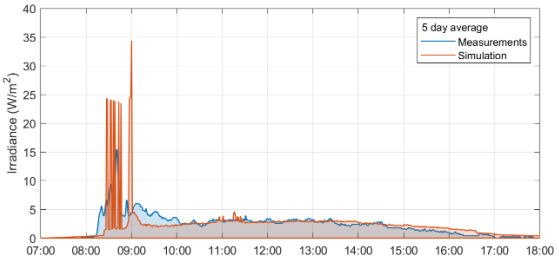

Figure 7: Office comparison simulation and measurement averages from a week in November

It can be seen that the two show a similar pattern. Only at the start of the day are deviations due to incidental shading apparent. This can be explained by small mismatches in the 3d models and solar position, which make the incident irradiance very sensitive during periods where sunlight directly enters the room. Also, mismatches between the simulated and real sky can cause for large deviations on a daily basis. However, these mismatches cancel each other out and on a weekly bases it can be observed that the daily solar irradiation has an absolute error below 10%.

3.3 Room characteristics analysis

With the approach explained in Section 2.4, the irradiation and PV energy yield are calculated. The results can be seen in Figure 8.

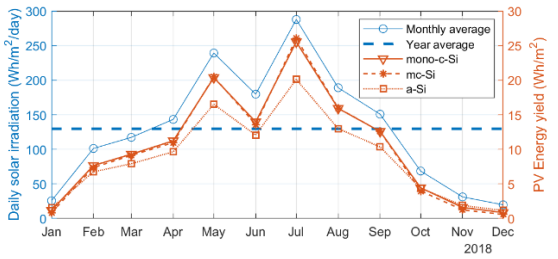

Figure 8: Office comparison simulation and measurement averages from a week in November

For the yearly simulations, the results show that the March equinox gives a good impression of the annual mean daily irradiation. This simplification was used to estimate annual mean daily irradiation for 20 different room characteristics of the two investigated rooms. The reduction in accuracy due to the simplification, can be overseen or now, as the results are only used to get a rough overview of suitable room characteristics. The results are shown in Figure 9.

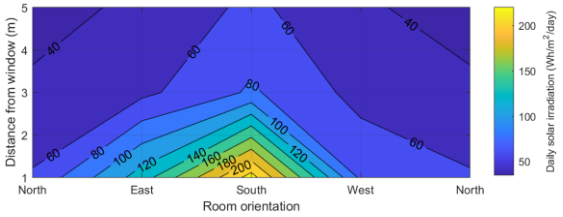

(a)

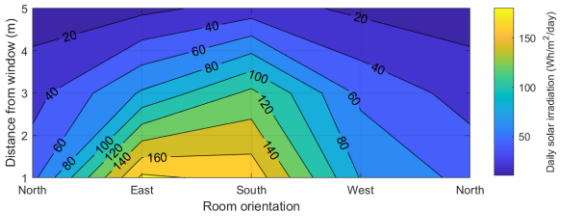

(b)

Figure 9: Average daily irradiation contour maps for the office (a) and household (b) model. The vertical axis of the map indicates the distance (in meters) of the sensor spot from the main room window at 1.8 meters from the floor (on the wall left of the main window). The horizontal axis shows the room orientation, which is defined as the direction of the main window normal vector pointing outside.

The figure can be used to find an estimation of the daily solar irradiation you can expect on the wall for a room in the Netherlands. For example, if you want to know the irradiation on the wall of the room you are sitting in, then first decide if its geometry and surroundings fit either the office room or the household room, then you need to know the direction the main window is facing, finally choose a spot on the wall at 1.8 meters from the floor and look up what value you can expect. Note, the results are on the wall on the left-hand side of the room only. This is why the peak is slightly between east and south. For the wall on the righthand side, one needs to mirror the contour map from left to right.

Using Equation 2.1, the converted PV energy yield can also be calculated for each of the cell technologies from Table 1. This is done again for all 20 different room characteristics and the results can be seen in Figure 10.

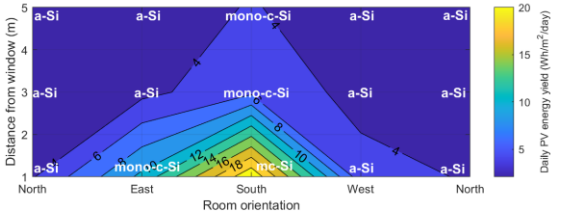

(a)

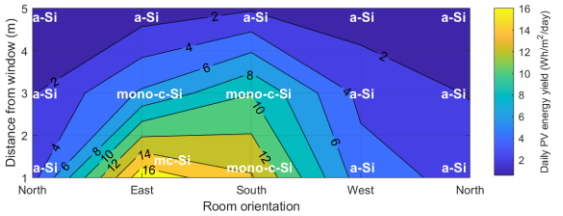

(b)

Figure 10: Average daily PV energy yield contour maps for the office (a) and household (b) model. The vertical and horizontal axis indicate the room characteristics, similar as described in the subscript of Figure 9. The white text, shows which technology performs best at each intersection of room characteristics and this PV technology is used to calculate the corresponding daily energy yield.

As can be expected, the contour maps look similar to those shown in Figure 9. The values now give an approximation of the converted PV energy yield that can be expected from a module in the corresponding room characteristics, as well as the best performing PV cell technology considered in this study.

4 PROTOTYPE

The results from the previous section are the foundation of three concept designs, corresponding to three different indoor light conditions. Only one concept, the *Window Winner* (WW), is developed more extensively and a prototype is created for further testing.

4.1 Design requirements

The Window Winner has been designed to be mobile, meaning you can move it around the room, but also take it out of its base and hang it on the wall. It needs to power a 2.4 W, warm light, LED strip for at least 1 hour on a daily basis. The size of the module is limited to 0.2 m^2 to keep it easy to displace. So, with an average daily consumption of 2.4 Wh, the WW needs at least 12 Wh/m^2/day. The target group will be an ordinary household, so looking more closely at Figure 10b, it can be seen that the direction of the main window should be no more than 90 degrees from south and within two meters from the main window. In this region monocrystalline silicon is the best performing cell technology.

It was decided to use interdigitated back contact (IBC) monocrystalline solar cells from SunPower [6], as the general opinion is that the lack of front contacts makes it easier to look at. Especially with a dark back sheet will the cells almost disappear in a black coloured product. Using a high system voltage will lower the current trough wires and components, hence, reduce resistive power losses to the square of the reduced current. On the other hand, the efficiency of DC/DC converters is less for larger voltage steps [7]. Thus, a 12 V system voltage has been chosen, largely also because of the wide availability of 12 V electrical components.

4.1 PV module design

For the PV module, five-inch SunPower monocrystalline IBC cells [6] were chosen for their performance and appearance. In total, 50 cells were cut into three pieces with a Fiber Laser Marking Machine. Current-Voltage (I-V) measurements were done on all cells, showing an average efficiency of 21.2% meaning the cells had lost only absolute 1% of efficiency during the cutting process. Further details and findings about the cutting process were used to set up a recipe for the cutting procedure of SunPower IBC cells. In total, 36 pieces of one third of a cell are connected in series using three bypass diodes. The product needs to be mobile, so a foil-to-foil lamination process was used to save weight. The module itself (without frame) has a weight of 1 kg/m^2.

4.2 The final product

The main components, shape and size of the Window Winner design can be seen in the engineering drawing of Figure 11.

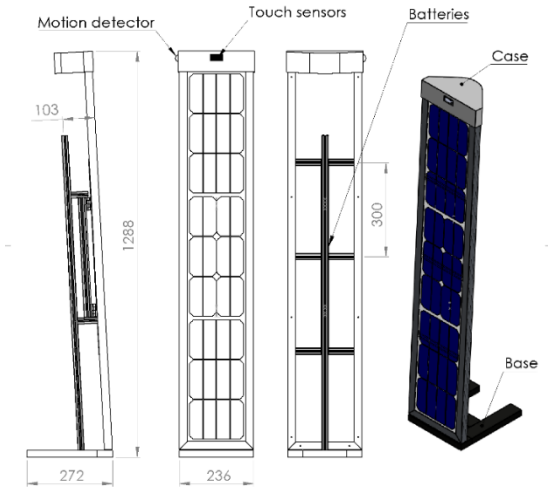

Figure 11: A engineering drawing of the indoor PV lamp. The main external components can be seen by the notes and only the most important dimensions are denoted. The motion detector is attached on the side and the touch sensor is on the front part of the casing. The batteries are incorporated in the frame.

A custom frame was created along with a case and base to support it. The module is connected to a suitable MPPT tracker and the converted energy is stored in a 12 V lithium battery pack during the day to be used for a 2.4 W white LED strip, placed on one side of the frame. Furthermore, an integrated pyroelectric infrared (PIR) motion sensor, light sensor and touch sensor switches are used to control the LED strip and assure a conservative use of the available energy. The final prototype can be seen in Figure 12.

Figure 12: A front (left) and back (right) image of the final version of the indoor PV lamp.

5 CONCLUSIONS

The aim of this paper was testing the feasibility of a mobile indoor photovoltaic lamp. A prototype has been built successfully for the two typical Dutch rooms investigated in this research. When staying in the designed position of the room, it can function without needing a charger. Before the design could be made, some research was performed to accurately determine the light conditions of the position where the device should operate. Near the window, the indoor irradiance coming from indirect sunlight during day time can range between 1 and 10 W/m^2. It was decided to neglect the influence of artificial light and only see it as a bonus if it contributes to the energy yield. For the office room, the sun only hits the wall directly in the morning hours, as can be seen in the simulation results from Figure 5. This is in accordance with the measurement results in Figure 4. On a daily basis the absolute error of the irradiation can lead to big deviations, due to mismatches in detected cloud cover and objects blocking the sun momentarily, such as leaves and blinds. But over the five-day period, these irregularities cancel each other out and the mean error decreases to only 10%. It was found that centimetre accuracy is required in the 3D model of the room, to account for minutes that the sun enters the room. Furthermore, a shorter time interval is needed for clearer skies. It was required to be as low as 1 minute when the sun hits the sensor directly, otherwise 1 hour is sufficient. When there is not much light in the indoor scene, the accuracy of the simulation needs to be higher, because of the nature of the backwards ray-tracing algorithm.

For the yearly simulations, the results showed that the March equinox gives a good impression of the annual average daily irradiation. This simplification was used to estimate annual average daily irradiation for 20 different room characteristics of the two investigated rooms. The resulting contour maps can be seen in Figures 9 and 10, along with the best performing cell technology. From these results, three working areas can be defined, corresponding to three investigated PV cell technology classes. For spots receiving high solar irradiation, multicrystalline silicon yields the most energy. But deeper into the room, or without a big window facing south, amorphous silicon can outperform the other technologies.

6 REFERENCES

[1] N. Tout, “The Pocket Calculator Race.” http://www.vintagecalculators.com, 2000-2019. Accessed: 2019-09-09.

[2] M. Muller, J. Wienold, W. D. Walker, and L. M. Reindl, “Characterization of indoor photovoltaic devices and light,” in 2009 34th IEEE Photovoltaic Specialists Conference (PVSC), pp. 738–743, IEEE, june 2009.

[3] R. Southall and F. Biljecki, “The VI-Suite: a set of environmental analysis tools with geospatial data applications,” Open Geospatial Data, Software and Standards, vol. 2, p. 23, dec 2017.

[4] CIE, “Spatial distribution of daylight - Luminance distributions of various reference skies.” https://www.techstreet.com/standards/cie-110-1994?product_id=1210128, 1994. Accessed: 2018-09-17.

[5] J. F. Randall, Designing indoor solar products : photovoltaic technologies for AES. J. Wiley & Sons, 2005.

[6] SUNPOWER, “C60 Solar Cell: Mono crystalline silicon,” tech. rep., 2010.

[7] N. Mohan, T. M. Undeland, and W. P. Robbins, Power Electronics: converters, applications, and design. John Wiley & Sons, 3 ed., 2003.